DOI: 10.1021/ma900554k

Macromolecules
ARTICLE

Synthesis and Characterization of Amphiphilic Multiblock Copolymers: Effect of the Number of Blocks on Micellization

Natalie A. Hadjiantoniou,[†] Aggeliki I. Triftaridou,[‡] Demetris Kafouris,[†] Michael Gradzielski,[§] and Costas S. Patrickios*,[†]

[†]*Department of Chemistry, University of Cyprus, P.O. Box 20537, 1678 Nicosia, Cyprus,* [‡]*Matière Molle et Chimie, ESPCI ParisTech-CNRS, UMR 7167, 10 Rue Vauquelin, 75231 Paris, Cedex 05, France, and* [§]*Stranski-Laboratorium für Physikalische and Theoretische Chemie, Institut für Chemie, Strasse des 17. Juni 124, Sekr. TC7, Technische Universität Berlin, D−10623 Berlin, Germany*

Received March 14, 2009; Revised Manuscript Received June 23, 2009

ABSTRACT: Five linear amphiphilic multiblock copolymers based on 2-(dimethylamino)ethyl methacrylate ("D") and methyl methacrylate ("M"), bearing from two to six blocks, were synthesized using sequential group transfer polymerization. All copolymers were obtained from the same polymerization flask (by the withdrawal of a sufficient amount of sample and appropriate adjustment of subsequent monomer loadings) to ensure better comparison between the various multiblocks. A theoretical degree of polymerization (DP_{th}) of 20 was targeted for all D blocks, whereas a DP_{th} of 10 was aimed for the M blocks. Upon characterization using gel permeation chromatography and ^{1}H NMR spectroscopy, the copolymers were confirmed to have the expected values of molecular weights and compositions. Subsequently, the aqueous micellization behavior of these copolymers was probed using dye solubilization, dynamic light scattering, and small-angle neutron scattering. Dye solubilization experiments indicated that micelles readily formed at low copolymer concentrations equal to or less than 0.03% w/w. The scattering measurements revealed that despite the differences in their overall DP_{th} values, the triblock, the tetrablock, and the pentablock copolymers self-assembled in water to form micelles with radii of gyration and hydrodynamic radii very similar to each other, suggesting chain looping and the formation of flowerlike micelles, which is in agreement with recent Monte Carlo simulations.

Introduction

Amphiphilic block copolymers are advanced surfactants with improved solubilization and stabilization properties and increasing importance in technology and medicine.[1] Most studies to date involve diblock and ABA triblock copolymers. There are also an increasing number of investigations on amphiphilic multiblock copolymers, but most of these concern poorly defined multiblock copolymers involving copolymer mixtures with a broad distribution in the number of blocks as a result of the stepwise oligomerization reactions employed for block interconnection.[2] In addition to the length heterogeneity, there is, in some cases, extensive topological heterogeneity because of the random placement of the two types of segments and the absence of block alternation arising from the lack of selectivity in the interconnection reaction.[3]

Contrary to the lack of well-defined water-compatible multiblock copolymers, there is sizable literature on hydrophobic multiblock copolymers that are used for bulk morphology studies.[4] Most of these investigations employ sequential anionic "living" polymerization, sometimes combined with chain dimerization to double the chain length, to prepare multiblock copolymers with up to 11 blocks. These materials display strict block alternation, high molecular weights (MWs), narrow molecular weight distributions (MWDs), and well-defined compositions.

In the present study, we report the preparation, for the first time, of well-defined amphiphilic multiblock copolymers via sequential multiple monomer addition. A special type of anionic polymerization was used for the synthesis. In particular, we employed group transfer polymerization (GTP),[5,6] which is best-suited for the polymerization of methacrylates. Methyl methacrylate ("M") was used as the hydrophobic monomer, whereas 2-(dimethylamino)ethyl methacrylate ("D") served as the hydrophilic, pH- and temperature-responsive comonomer. Five multiblock copolymers were prepared, bearing two, three, four, five, and six blocks. After confirmation of their MWs and composition, all amphiphilic multiblock copolymers were characterized in terms of their aqueous micellization properties using a host of techniques to determine their critical micellization concentrations (cmc's), aggregation numbers (N_{agg}), radii of gyration (R_g), and hydrodynamic radii (R_h).

*To whom correspondence should be addressed. E-mail: costasp@ucy.ac.cy.

Experimental Section

Materials and Methods. The monomers, "D" (98%) and "M" (99%), the initiator, 1-methoxy-1-(trimethylsiloxy) methyl propene (MTS, 95%), basic alumina, calcium hydride (CaH_2, 90−95%), and 2,2-diphenyl-1-picrylhydrazyl hydrate (DPPH, 95%) were all purchased from Aldrich, Germany. Deuterated chloroform ($CDCl_3$) was purchased from Merck, Germany. Tetrahydrofuran (THF, 99.8%, both HPLC and reagent grade) was purchased from Labscan, Ireland.

The D and M monomers were passed through basic alumina columns to ensure that any acidic impurities were removed. They were subsequently stirred overnight over CaH_2 in the presence of the free radical inhibitor DPPH to neutralize any traces of water or other protonic impurities and were finally freshly distilled prior to use. The initiator, MTS, was also freshly distilled prior to use. The solvent, THF, was dried by being

 Published on Web 07/17/2009

refluxed over a sodium/potassium alloy for 3 days and was freshly distilled. Tetrabutylammonium bibenzoate (TBABB) was the polymerization catalyst and was prepared as described by Dicker and coworkers[6] and stored under vacuum until use.

Polymer Synthesis. The polymers were synthesized using GTP. In total, six polymers were synthesized: one of them was the homopolymer of the hydrophilic D, and the others were copolymers of D and the hydrophobic M, bearing from two up to six blocks. All D-blocks had a theoretical degree of polymerization (DP_{th}) equal to 20, and all M-blocks had a DP_{th} equal to 10. The preparation of the (co)polymers was accomplished by sequential monomer additions. All polymers of this study were obtained from the same reaction flask and by extracting enough sample, which was subsequently precipitated in *n*-hexane and vacuum-dried at room temperature. This procedure was elected to ensure absolutely identical blocks in the copolymers. To bypass the problem arising from uncertainties in the densities of the (co)polymer solutions in the various stages of the polymerization and to ensure the addition of the correct amount of monomer in each stage, the exact mass of the polymer solution extracted each time was determined gravimetrically, and from that the monomer quantity necessary to be added for the next stage was calculated with the aid of a preconstructed spreadsheet.

The procedure is detailed below. Freshly distilled THF (90 mL) was transferred using a glass syringe to a 250 mL round-bottomed flask preloaded with a small amount of TBABB catalyst, followed by the addition of 1.1 mL (0.94 g, 5.4 mmol) of MTS initiator. Then, 17.7 mL (16.5 g, 105 mmol) of D monomer was added dropwise under stirring. The polymerization exotherm (23.4−37.7 °C) abated within 5 min; a sample (0.2 mL) for gel permeation chromatography (GPC) and ^{1}H NMR spectroscopy was extracted, and also 31.0 mL (29.03 g) of the reaction solution was extracted to obtain 4.9 g of D homopolymer (monomer conversion = 100%; polymer number-average MW = M_n = 3790 g mol^{-1}; polydispersity index = PDI = M_w/M_n = 1.10; M_w is the weight-average MW). Following that, 3.9 mL (3.66 g, 36.5 mmol) of M monomer was added, producing an exotherm (27.1−33.1 °C). After extracting a small sample (0.2 mL) of the solution of the formed D_{20}-*b*-M_{10} diblock copolymer for GPC (monomer conversion = 100%; M_n = 5270 g mol^{-1}; PDI = 1.11) and ^{1}H NMR spectroscopy (found 37.0% mol M compared with 33.3% theoretically expected) analyses and another 24.5 mL (24.44 g) solution for recovering 5.2 g of diblock copolymer, 8.3 mL (7.74 g, 49.3 mmol) of D monomer was added, leading to the formation of the D_{20}-*b*-M_{10}-*b*-D_{20} triblock copolymer. Again, a small sample (0.2 mL) of the formed triblock copolymer was extracted for GPC (monomer conversion = 100%; M_n = 8360 g mol^{-1}; PDI = 1.21) and ^{1}H NMR spectroscopy (found 21.6% mol M compared with 20.0% theoretically expected) analyses, followed by the extraction of another 15.6 mL (15.24 g) of polymerization solution for recovering 4.9 g of triblock copolymer. With further similar additions, the tetrablock, the pentablock, and the hexablock copolymers were obtained. In particular, for the synthesis of the D_{20}-*b*-M_{10}-*b*-D_{20}-*b*-M_{10} tetrablock copolymer, 1.9 mL of M monomer (1.78 g, 17.6 mmol) was added, and then 14.2 mL (13.78 g) of solution was extracted (monomer conversion = 100%; M_n = 9140 g mol^{-1}; PDI = 1.24; found 29.6% mol M compared with 33.3% theoretically expected). Furthermore, the synthesis of the D_{20}-*b*-M_{10}-*b*-D_{20}-*b*-M_{10}-*b*-D_{20} pentablock copolymer was accomplished by the addition of 3.9 mL of D monomer (3.64 g, 23.2 mmol) and the extraction of 11.4 mL (11.22 g) of the polymerization solution (monomer conversion = 100%; M_n = 11 400 g mol^{-1}; PDI = 1.38; found 21.5% mol M compared with 25.0% theoretically expected). Finally, the D_{20}-*b*-M_{10}-*b*-D_{20}-*b*-M_{10}-*b*-D_{20}-*b*-M_{10} hexablock copolymer was obtained by the addition of 0.8 mL of M monomer (0.75 g, 7.2 mmol) (monomer conversion = 100%; M_n = 11 900 g mol^{-1}; PDI = 1.52; found 28.9% mol M compared with 33.3% theoretically expected).

Polymer Characterization. *Gel Permeation Chromatography and Proton Nuclear Magnetic Resonance Spectroscopy.* The samples extracted during the various stages of the polymerization were characterized in terms of their MWs and composition using GPC and ^{1}H NMR spectroscopy analyses, respectively. GPC was performed at room temperature on a Polymer Laboratories system equipped with a Waters 515 isocratic pump, an ERC-7515A Polymer Laboratories refractive index (RI) detector, and a PL Mixed "D" column (bead size of 5 μm and bead pore sizes of 10, 50, 100, and 1000 nm). The eluent was THF, delivered at 1 mL min^{-1}. The calibration of the instrument was made using polyM MW standards supplied by Polymer Laboratories. A 300 MHz Avance Bruker spectrometer equipped with an Ultrashield magnet was used for recording the ^{1}H NMR spectra of the polymers in $CDCl_3$. The copolymer composition was calculated from the ratio of the area of the resonance due to the two oxymethylene protons of polyD at 4.0 ppm to the area of the resonance due to the three methoxy protons of polyM at 3.6 ppm.

Hydrogen Ion Titration. Solutions of each polymer (5 g of 1% w/w solutions) were titrated in the pH range from 2 to 12 using a 0.5 N NaOH standard solution. The pH of the solution was measured using a Corning PS30 pH meter. The effective pK values of the D-units were calculated as the corresponding pH values at 50% ionization. The pH at which any polymer precipitation occurred during the titration was also noted.

Turbidimetry. The cloud points of 1% w/w (co)polymer solutions were determined using turbidimetry. Two groups of measurements were obtained: one in which the solvent was pure water, which, however, did not include the hexablock copolymer because of its insolubility in that solvent, and one which covered all (co)polymers by using a 70:30 v/v water/THF solvent mixture. In the latter case, the (co)polymer was first dissolved in THF, and the resulting solution was diluted in the appropriate volume of water. A Lambda 10 UV−vis spectrophotometer from Perkin-Elmer was used for the turbidity measurements. The polymer solutions were placed in a quartz cuvette with a path length of 10 mm and kept under stirring during the measurement. A small temperature sensor was immersed in the heated solution. The optical density at 500 nm and the temperature were measured using the TempLab (version 1.56) software. The cloud point was determined to be the temperature at which the optical density presented the first abrupt increase.

Dye Solubilization. Aqueous copolymer solutions of eleven different concentrations, varying between 5×10^{-6} and 0.5% w/w for each copolymer, containing 1 M NaCl and adjusted at pH ∼3, were prepared, and an equal volume of an aqueous solution of pyrene was added to each copolymer solution so that the final concentration of pyrene became 5×10^{-7} M. Subsequently, the absorbance of the copolymer solutions with the pyrene was measured within the range 500−300 nm using a UV-1601 Shimadzu spectrophotometer.

Dynamic Light Scattering. Aqueous copolymer solutions of concentration 1% w/w in the presence of 1 M NaCl at pH ∼3 were characterized in terms of their hydrodynamic radius by dynamic light scattering (DLS) using a 90Plus Brookhaven spectrophotometer with Particle Sizing Software version 2.31, equipped with a 30 mW red diode laser operating at 673 nm. The measurements were performed at an angle of 90° and at room temperature. The data were processed using multimodal size distribution analysis based on non-negatively constrained least-squares (NNCLS). Prior to the light scattering measurements, the polymer solutions were filtered using PTFE filters with 0.45 μm pore diameters and were left to settle for about 1 h so that any air bubbles could escape.

Small-Angle Neutron Scattering. The radii of gyration, R_g, and the absolute M_w of the micelles formed by the multiblock copolymers in 1% w/w solutions in D_2O containing 1 M NaCl at pH ∼3 were measured using small-angle neutron scattering (SANS). The measurements were carried out at the Laboratoire

Léon Brillouin (LLB) at the CEA-CNRS in Saclay, France, using the PAXE spectrometer. A neutron wavelength of 6 Å and sample-to-detector distances of 1.055 and 4.055 m were employed, thereby covering a range of magnitude of the scattering vector, q, of 0.009 to 0.33 Å^{-1}. The solutions of the copolymers were contained in Hellma quartz cuvettes of 2 mm thickness. The sensitivity of the individual detector elements was accounted for by a comparison with the scattering of a water sample in a 1 mm thickness quartz cuvette. The data were recorded on a 64 × 64 2D detector, subsequently radially averaged, corrected for the transmission values, and converted into absolute scattering intensities by comparison with the intensity of the incident beam via a standard procedure.[7] The background scattering of the empty cell and the electronic background were subtracted during this procedure. The analysis of the SANS data was done by fitting the model of the Gaussian starlike polymers[8] to the whole scattering curve $I(q)$ to obtain R_g and M_w. For this model, the scattering intensity is given by eq 1

$$I(q) = c_g \frac{M_w}{N_{AV}\rho^2}(\rho_p - \rho_s)^2 \times \frac{2}{fx^2}\left[x - (1 - e^{-x}) + \frac{f-1}{2}(1 - e^{-x})^2\right] + I_{inc} \qquad (1)$$

$$x = \frac{f}{3f-2} q^2 R_g^2$$

Here c_g is the mass concentration of the copolymer, N_{AV} is Avogadro's constant, ρ is the density of the polymer taken to be equal to 1.19 g mL^{-1}, ρ_p and ρ_s are the scattering length densities of the polymer and the solvent, respectively, and f is the number of arms in the star model, which, in our case, was associated with the aggregation number N_{agg} of the micelle, which is given by the ratio M_w (micelle)/M_n (chain). Finally, I_{inc} is the constant incoherent background scattering that mostly arises from the H atoms present in the samples. For ρ_s, we employed the value of deuterium oxide of 6.37×10^{10} cm^{-2}. The ρ_p values were polymer-specific and were calculated from the copolymer composition and by using homopolymer ρ_p values of 8.23×10^9 and 10.5×10^9 cm^{-2} for polyD and polyM, respectively. The thus-calculated copolymer ρ_p values range between 8.55×10^9 and 8.77×10^9 cm^{-2}. At this point, we wish to stress that the Gaussian starlike polymer model does not truly represent the detailed structure of the aggregates, but this simple model captures the essential aspects of the block copolymer micelles, that is, a scattering length density that decreases continuously when moving away from the center and a Gaussian behavior at larger q. Therefore, this model is superior to the simple sphere or core−shell models. Fits of comparable or better quality are only obtained for models with a more refined shell structure, such as the Pedersen−Gerstenberg model.[9] However, for our purposes of obtaining N_{agg} via M_w and some characteristic measure of the size of the aggregates, our preliminary evaluation by means of the starlike polymer model is sufficient. Further more detailed modeling of the scattering data to obtain a more refined structural picture of the aggregates is in progress.

Results and Discussion

Polymerization Methodology. The chemical structures of the monomers and the initiator are given in Figure 1, whereas the structures of all synthesized polymers are presented in Figure 2. The procedure followed for the preparation of the hexablock copolymer is illustrated in Figure 3. Although the syntheses of diblock[10−12] and ABA triblock[13] copolymers of D and M have previously been reported, the preparation of higher multiblocks has yet to be reported. The synthesis of the (co)polymers of the present study was performed via

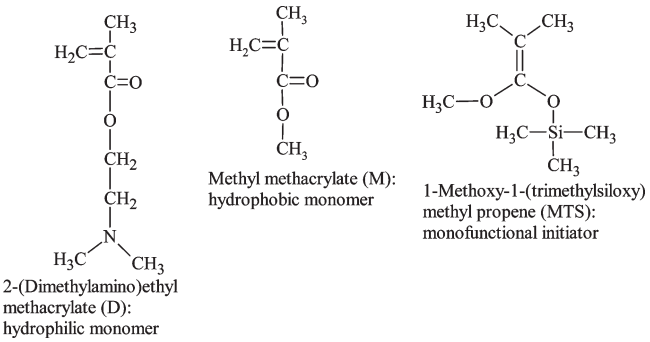

Figure 1. Chemical structures and names of the monomers and the initiator used for the polymerizations.

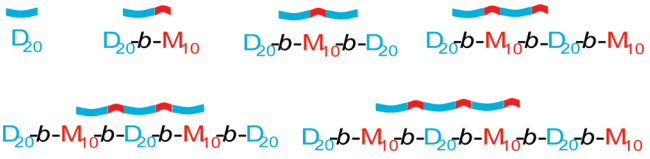

Figure 2. Structures of all linear (co)polymers synthesized. D: 2-(dimethylamino)ethyl methacrylate; M: methyl methacrylate.

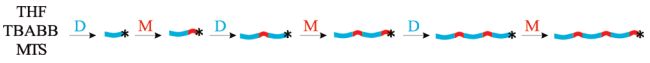

Figure 3. Synthetic procedure followed for the synthesis of the hexablock copolymer. THF: tetrahydrofuran; TBABB: tetrabutylammonium bibenzoate; MTS: 1-methoxy−1-(trimethylsiloxy) methyl propene; D: 2-(dimethylamino)ethyl methacrylate; M: methyl methacrylate.

sequential monomer additions in a single flask, from which all (co)polymers were obtained. The first step resulted in the preparation of the D_{20} homopolymer, having the one end active (indicated by an asterisk in Figure 3). The second step led to the synthesis of the D_{20}-*b*-M_{10} diblock copolymer, again with one active end. Further sequential monomer additions provided the other multiblock copolymers with greater numbers of blocks but the same DP_{th} values in the corresponding blocks.

The chosen synthetic strategy had two implications for the molecular characteristics of the resulting (co)polymers. First, copolymers with more blocks had a greater DP_{th} and higher MW. Second, all copolymers with an even number of blocks had the same percentage of hydrophobic units, which was greater than that of the copolymers with an odd number of blocks; the hydrophobic composition of the latter type of block copolymers increased with the number of blocks. (See the following paragraph and Table 1.)

Polymer Molecular Weights and Compositions. The M_n values, the peak MW, M_p, values (MWs at the peak maximum), and the compositions of the copolymers as measured by GPC and ^{1}H NMR spectroscopy are shown in Table 1. Figure 4 presents the GPC traces of all (co)polymers. The M_n values were close to the theoretically expected MWs calculated from the monomer/initiator feed ratios. The MWDs were relatively narrow with PDIs, in most cases, lower than 1.4 and higher (ca. 1.5) only for the hexablock copolymer. The higher PDIs of the higher multiblocks are probably due to the higher copolymerization solution viscosities and the multiple sampling. The percentage compositions determined from ^{1}H NMR spectroscopy were close to those expected theoretically on the basis of the comonomer feed ratios, confirming full monomer-to-polymer conversion during synthesis. The M content in the copolymers

Table 1. Molecular Weights and Compositions of the (Co)polymers of This Study

no.	polymer structure[a]	theor MW[b]	GPC results			M (mol %)	
			M_n	M_w/M_n	M_p	theory	^{1}H NMR
1	D_{20}	3241	3790	1.10	4390	0	0
2	D_{20}-*b*-M_{10}	4241	5270	1.11	6080	33.3	37.0
3	D_{20}-*b*-M_{10}-*b*-D_{20}	7381	8360	1.21	11 400	20.0	21.6
4	D_{20}-*b*-M_{10}-*b*-D_{20}-*b*-M_{10}	8381	9140	1.24	12 400	33.3	29.6
5	D_{20}-*b*-M_{10}-*b*-D_{20}-*b*-M_{10}-*b*-D_{20}	11 521	11 400	1.38	19 400	25.0	21.5
6	D_{20}-*b*-M_{10}-*b*-D_{20}-*b*-M_{10}-*b*-D_{20}-*b*-M_{10}	12 521	11 900	1.52	22 500	33.3	28.9

[a] D: 2-(dimethylamino)ethyl methacrylate; M: methyl methacrylate. [b] Contribution from the initiator fragment of 101 g mol^{-1} was included in the calculation.

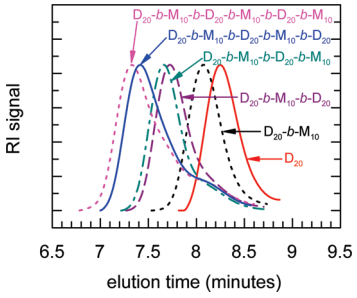

Figure 4. Gel permeation chromatograms of all (co)polymers of this study prepared by sequential group transfer polymerization. D: 2-(dimethylamino)ethyl methacrylate; M: methyl methacrylate.

was kept relatively low, at 33 mol % or lower, to secure the water solubility of the (co)polymers.

Effective p*K* Values and Precipitation pH Values. Table 2 shows the effective p*K* values of the D-monomer repeating units and the pH values of precipitation of the (co)polymers, as determined using hydrogen ion titration. The effective p*K* values of the D units in all (co)polymers were determined to be around 7, which is in agreement with previous investigations on linear polymers containing D segments.[14] During titrations, precipitation of the diblock, the tetrablock, and the hexablock copolymers occurred. The homopolymer, the triblock, and the pentablock copolymers did not precipitate during titration because of their higher content in the hydrophilic D monomer. The pH at which precipitation was observed for the three block copolymers is also listed in Table 2.

Polymer Cloud Points. The cloud points of all (co)polymers are plotted in Figure 5 against the number of blocks. In Figure 5, the mol % D experimental composition of the (co)polymers is also presented as a function of the number of blocks. A general feature of these plots is that each cloud point versus number of blocks curve followed the corresponding mol % composition in D of the (co)polymers versus number of blocks curve, with the homopolymer of D presenting the highest cloud point, confirming the importance of polymer composition for its cloud point. This was expected because D is hydrophilic, and copolymers richer in D should precipitate at higher temperatures. The cloud points of copolymer solutions in 70:30 v/v water/THF mixtures were approximately 5 °C higher than those in pure water.

The present results on the polymer cloud points were important for choosing the most appropriate aqueous environment for the subsequent characterization of the micellar properties of the multiblock copolymers. Pure water was excluded because this could not dissolve the highest multiblock; furthermore, the cloud points of the lower homologues in this solvent were too close to room temperature. Although the presence of an organic solvent could sufficiently enhance the copolymer aqueous solubility, this

Table 2. Effective p*K* Values of the D Monomer Repeating Units and pH Values of Precipitation of the (Co)polymers As Determined by Hydrogen Ion Titration

no.	polymer structure[a]	pH of precipitation	p*K*
1	D_{20}		7.15
2	D_{20}-*b*-M_{10}	10.35	7.05
3	D_{20}-*b*-M_{10}-*b*-D_{20}		7.12
4	D_{20}-*b*-M_{10}-*b*-D_{20}-*b*-M_{10}	11.07	7.10
5	D_{20}-*b*-M_{10}-*b*-D_{20}-*b*-M_{10}-*b*-D_{20}		7.11
6	D_{20}-*b*-M_{10}-*b*-D_{20}-*b*-M_{10}-*b*-D_{20}-*b*-M_{10}	11.01	7.00

[a] D: 2-(dimethylamino)ethyl methacrylate; M: methyl methacrylate.

was avoided because of the high volatility of organic solvents such as THF. Instead, solubility enhancement was pursued via the full ionization of the D units at pH ~3. However, to suppress the intense intermolecular Coulombic repulsion in this highly charged system, which might disrupt micellization, the addition of 1 M NaCl was employed.

Critical Micellization Concentration. The maximum absorbance of pyrene (wavelength range of λ_{max} = 334.2 to 337.4 nm) in copolymer solutions of various concentrations was plotted against the copolymer concentration. As the copolymer concentration increased, an increase in pyrene absorbance was observed because of the tendency of the hydrophobic pyrene to partition in a nonpolar environment, which was provided by the core of the micelles being formed. The cmc was estimated to be the copolymer concentration at which the first increase in absorbance occurred.[15] Figure 6 presents the base 10 logarithm of the cmc's (in % w/w) as a function of the number of blocks. The $\log_{10}$(cmc) values fluctuated with the number of blocks, presenting a trend similar to that observed in Figure 5 for the cloud points. In fact, the more hydrophobic diblock, tetrablock, and hexablock copolymers exhibited lower cmc values than their triblock and pentablock homologues.

A power-law expression for $\log_{10}$(cmc) with respect to the experimental mol % M content and the M_n value[16] was fitted to the data for all multiblock copolymers. Nonlinear regression provided the optimal exponents and constant, as given in eq 2 below

$$\log_{10}(\text{cmc}) = -9.7 \times 10^{-3} \times (\text{mol \% M})^{1.19} \times M_n^{0.15} \quad (2)$$

whereas the regressed values are also plotted in Figure 6 with satisfactory agreement with the experimental values. Equation 2 suggested that $\log_{10}$(cmc) decreased both with the hydrophobic content and with the overall MW, as expected. However, this decrease was about eight times faster with the former than the latter, highlighting the greater importance of hydrophobicity for the onset of micellization.

Micellar Sizes. The results on the micellar sizes, as determined by SANS and DLS, are listed in Table 3 and plotted in Figure 7, whereas schematic representations of the micellar structures drawn on the basis of these data are illustrated in Figure 8. The R_g and N_{agg} values were calculated

from SANS, whereas the R_h values were obtained from DLS. The maximum possible micelle radius, R_{max}, was also calculated from the fully stretched relevant portion of the copolymer chain; in this calculation, the M_n values from GPC were used.

We present our findings by focusing first on the micellar radii, and, in particular, on the R_g and R_h families of data in Figure 7. In this Figure, the R_h values were higher than the R_g values for all block copolymers, with the R_h/R_g ratio being equal to or somewhat higher than the value for compact spheres, indicating the high compactness of the present micelles. Both families of data presented the same trends with respect to the number of blocks. First of all, the most striking observation was the almost constant R_g and R_h values of the micelles formed by the triblock, the tetrablock, and the pentablock copolymers. Second, the micelles formed by the diblock copolymer exhibited R_g and R_h values that were 50% higher than those of the triblock, the tetrablock, and the pentablock copolymers. Finally, the micelles formed by the hexablock copolymer displayed the highest R_g and R_h values, which were approximately twice as high as those presented by the micelles formed by the triblock, the tetrablock, and the pentablock copolymers.

We start our discussion on the trends in the R_g and R_h values by first explaining the differences between the micelles

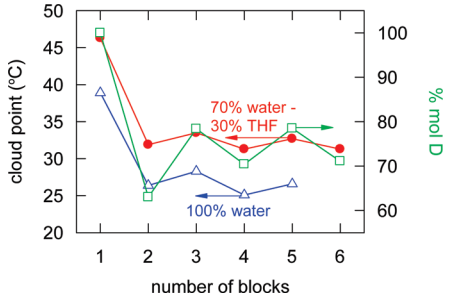

Figure 5. Cloud points in pure water and in water/tetrahydrofuran (THF) 70:30 v/v mixtures at 1% w/w copolymer concentration as well as the mol % experimental composition in 2-(dimethylamino)ethyl methacrylate (D) as a function of the number of blocks of all (co)polymers.

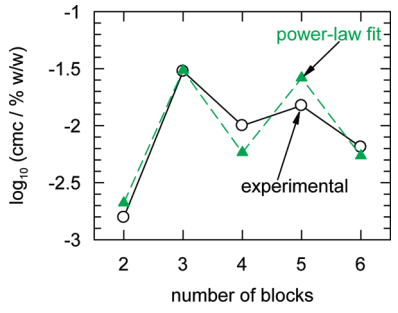

Figure 6. Critical micellization concentrations (cmc's) of all copolymers as a function of their number of blocks.

formed by the diblock and the triblock copolymers. To a first approximation, one would expect the size of spherical micelles formed by a diblock copolymer to be the same as that of spherical micelles formed by an ABA triblock copolymer (with a solvophobic midblock B) when the latter is the dimer of the aforementioned diblock ("AB-diblock-" vs "ABA-triblock-" copolymer-type micelles). However, this was not exactly the case here: although the ABA triblock copolymer had two similar hydrophilic A blocks, each of which was of the same DP_{th} as that of the hydrophilic block of the diblock, the solvophobic B midblock of the triblock was not twice the size of the diblock but was of exactly the same size. Therefore, the contour length of the diblock, calculated from its M_n to be 9.8 nm, which would represent an upper bound for the micellar radius, was greater than half the contour length of the triblock, estimated to be 7.4 nm, corresponding to the maximum micellar radius. These values are also plotted in Figure 7 in the R_{max} family of data and are indicated using arrows in Figure 8. In addition to the differences in the appropriate contour lengths, there was greater chain stretching in the micelles formed by the diblocks as a result of their greater aggregation numbers arising from their higher hydrophobicity than the ABA triblocks. Both of these factors as well as entropic factors led to the greater micellar radii of the diblocks than the ABA triblocks despite the greater unimer MW of the latter than the former.

Our experimental finding that the micelles of the triblock, the tetrablock, and the pentablock copolymers all displayed the same radii implies folding of the chains of the tetrablock and the pentablock copolymers in their micelles, as indicated schematically in Figure 8. Therefore, in these three block copolymers, the maximum micellar radius was defined by the same contour length, comprising one hydrophilic block plus one-half hydrophobic block, adding up to about 7 nm. The entropically unfavorable loop formation[17] in the tetrablock and the pentablock copolymers (one loop per chain) was sufficiently counterbalanced by the large hydrophobic driving force for micellization in this strongly segregated system.[18] Significantly, a weak dependence of the radius of

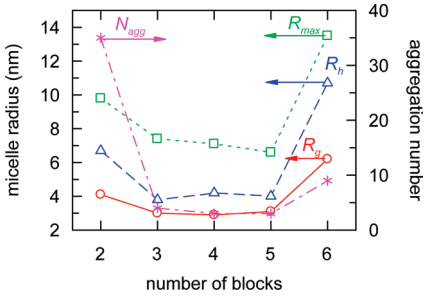

Figure 7. Dependence of micellar radii R_g, R_h, and R_{max} and aggregation numbers, N_{agg}, on the number of blocks of the amphiphilic multiblock copolymers in aqueous solution.

Table 3. Radii of Gyration, Hydrodynamic Radii, Maximum Radii, Weight-Average Molecular Weights, and Aggregation Numbers of the Micelles Formed by the Multiblock Copolymers in Aqueous Solution[a]

no.	polymer structure[b]	R_g (nm) (SANS)	R_h (nm) (DLS)	R_{max} (nm)	$M_{w,micelle}$ (g mol^{-1}) (SANS)	$M_{n,unimer}$ (g mol^{-1}) (GPC)	$N_{agg} = M_{w(SANS)}/M_{n(GPC)}$
2	D_{20}-*b*-M_{10}	4.1	6.7	9.8	182 000	5270	34.5
3	D_{20}-*b*-M_{10}-*b*-D_{20}	3.0	3.8	7.4	33 100	8360	3.9
4	D_{20}-*b*-M_{10}-*b*-D_{20}-*b*-M_{10}	2.9	4.2	7.1	30 500	9140	3.3
5	D_{20}-*b*-M_{10}-*b*-D_{20}-*b*-M_{10}-*b*-D_{20}	3.1	4.0	6.6	33 000	11 400	2.9
6	D_{20}-*b*-M_{10}-*b*-D_{20}-*b*-M_{10}-*b*-D_{20}-*b*-M_{10}	6.2	10.7	13.5	119 000	11 900	9.0

[a] Number-average molecular weights of the unimers are also provided. [b] D: 2-(dimethylamino)ethyl methacrylate; M: methyl methacrylate.

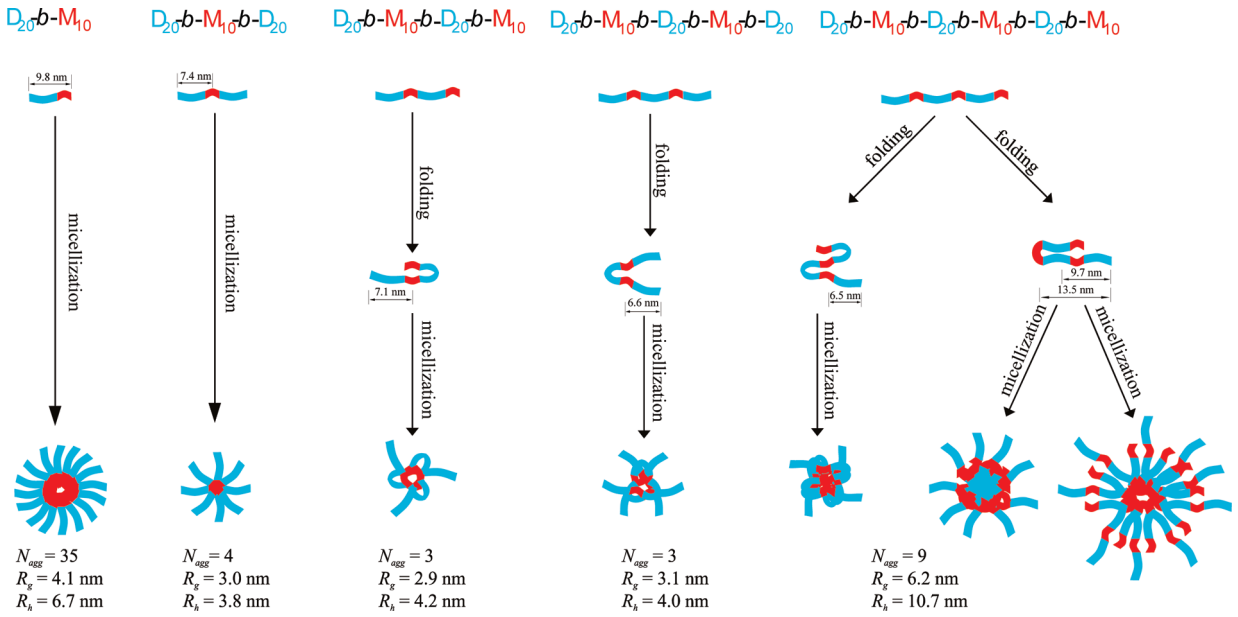

Figure 8. Proposed structures of the micelles formed by the multiblock copolymers in aqueous solution. For the higher multiblocks (tetrablock and above), the folded conformation of an individual copolymer chain as encountered in the micelles is also shown. For the highest multiblock, the hexablock, two different folded chain conformations, and three different possible micellar structures are shown. The experimental micellar aggregation numbers, N_{agg}, and micellar radii, R_g and R_h, are indicated for each multiblock copolymer.

gyration of micelles formed by amphiphilic multiblock copolymers with strictly alternating blocks in selective solvents on the number of blocks is predicted in recent Monte Carlo simulations.[19]

Finally, the values of R_g and R_h of the micelles formed by the hexablock copolymer were not equal but were higher (by a factor of two) than those formed by the three immediately lower multiblocks. If the former micelles were to display the same radii as the latter, then this would require that each hexablock copolymer chain form two folds in its micelles (Figure 8), which, apparently, was entropically very demanding. In contrast, the measured R_g and R_h values were more consistent with one fold per chain, leading to the larger and compartmentalized micelle structures also depicted in Figure 8.

Now, turning our attention to N_{agg}, in Figure 7 the aggregation numbers qualitatively exhibited the same dependence on the number of blocks as the micellar radii. This was in agreement with our expectation that larger micelles would present both larger radii and greater aggregation numbers, and it further implied that all micelles had approximately the same compactness, which is consistent with their similar R_h/R_g ratios noted above.

Conclusions

GTP was employed for the preparation of five amphiphilic multiblock copolymers of D and M, bearing up to six blocks. Each higher multiblock contained an extra block but shared all previous blocks with its lower homologues. After confirming that all polymers had the proper molecular weights and compositions, water solubility studies indicated that the cloud points of neutral multiblock copolymers were just above room temperature, and this solubility substantially increased upon ionization of the hydrophilic D blocks. Subsequently, the aqueous micellization properties of the ionized copolymers were investigated using a host of techniques. Pyrene solubilization experiments showed that micellization readily took place in all cases at low copolymer mass concentrations. Small-angle neutron and light scattering experiments allowed the calculation of the micellar aggregation numbers, the radii of gyration, and the hydrodynamic radii. The micellar radii were sufficiently small and of the same value for the micelles formed by the triblock, the tetrablock, and the pentablock copolymers, suggesting that the chains of the tetrablocks and the pentablocks folded once in the respective micelles. The radii of the micelles formed by the hexablock copolymer were greater than those of its three immediately lower homologues, excluding the possibility for two folds per chain in the micelles of the former copolymer but rather suggesting again one loop per chain and thereby forming correspondingly larger particles with additional shells.

Future work will aim at examining the validity of the conclusions of this work for other multiblock copolymer systems. In particular, systems with different relative block sizes (preferably larger) and also different monomer combinations will be prepared and characterized.

Acknowledgment. We thank the Cyprus Research Promotion Foundation for supporting this work in the form of a PENEK 2005 grant (project ENISX/05/05/19) to N.A.H. The Laboratoire Léon Brillouin (LLB), CEA-Saclay, France, and the European Commission are also thanked for funding the SANS experiments. The valuable and comprehensive help of Dr. Laurence Noirez of LLB with the SANS experiments is gratefully acknowledged. We also thank Professor Walther Burchard of the University of Freiburg, Germany, for his interest in our work and also for carrying out some complementary light scattering experiments for us. Similarly, we thank our colleague Professor Yachin Cohen of the Technion Israel Institute of Technology, Haifa, Israel, for performing some preliminary small-angle X-ray scattering and cryotransmission electron microscopy measurements on samples of the present system. Finally, we thank the A. G. Leventis Foundation for a generous donation that enabled the purchase of the NMR spectrometer of the University of Cyprus.

Supporting Information Available: SANS profiles of all block copolymers at 1% w/w polymer concentration in D_2O containing 1 M NaCl at pH ~3. This material is available free of charge via the Internet at http://pubs.acs.org.

References and Notes

(1) (a) Hadjichristidis, N.; Pispas, S.; Floudas, G. A. *Block Copolymers: Synthetic Strategies, Physical Properties, and Applications*; John Wiley & Sons: New York, 2002. (b) *Amphiphilic Block Copolymers: Self-Assembly and Applications*; Alexandridis, P., Lindman, B., Eds.; Elsevier: Amsterdam, 2000. (c) Hamley, I. W. *The Physics of Block Copolymers*; Oxford University Press: New York, 1998.

(2) (a) Wang, W. J.; Li, T.; Yu, T.; Zhu, F. M. *Macromolecules* **2008**, *41*, 9750–9754. (b) Sasaki, D.; Suzuki, Y.; Hagiwara, T.; Yano, S.; Sawaguchi, T. *Polymer* **2008**, *49*, 4094–4100. (c) Zhou, Y.; Jiang, K.; Song, Q.; Liu, S. *Langmuir* **2007**, *23*, 13076–13084.

(3) (a) You, Y.-Z.; Zhou, Q.-H.; Manickam, D. S.; Wan, L.; Mao, G.-Z.; Oupický, D. *Macromolecules* **2007**, *40*, 8617–8624. (b) Fang, H.; Zhou, S.; Wu, L. *Appl. Surf. Sci.* **2006**, *253*, 2978–2983. (c) Nagata, M.; Sato, Y. J. *Polym. Sci., Part A: Polym. Chem.* **2005**, *43*, 2426–2439.

(4) (a) Nagata, Y.; Masuda, J.; Noro, A.; Cho, D.; Takano, A.; Matsushita, Y. *Macromolecules* **2005**, *38*, 10220–10225. (b) Wu, L.; Cochran, E. W.; Lodge, T. P.; Bates, F. S. *Macromolecules* **2004**, *37*, 3360–3368. (c) Spontak, R. J.; Smith, S. D. J. *Polym. Sci., Part B: Polym. Phys.* **2001**, *39*, 947–955.

(5) (a) Webster, O. W.; Hertler, W. R.; Sogah, D. Y.; Farnham, W. B.; RajanBabu, T. V. *J. Am. Chem. Soc.* **1983**, *105*, 5706–5708. (b) Sogah, D. Y.; Hertler, W. R.; Webster, O. W.; Cohen, G. M. *Macromolecules* **1987**, *20*, 1473–1488. (c) Webster, O. W. *J. Polym. Sci., Part A: Polym. Chem.* **2000**, *38*, 2855–2860. (d) Webster, O. W. *Adv. Polym. Sci.* **2004**, *167*, 1–34.

(6) Dicker, I. B.; Cohen, G. M.; Farnham, W. B.; Hertler, W. R.; Laganis, E. D.; Sogah, D. Y. *Macromolecules* **1990**, *23*, 4034–4041.

(7) Cotton, J. P *Neutron, X-ray, and Light Scattering: Introduction to an Investigative Tool for Colloidal and Polymeric Systems*; Lindner, P., Zemb, P.H., Eds.; North-Holland, Amsterdam, 1991; p 19.

(8) Benoit, H. J. *Polym. Sci.* **1953**, *11*, 507–510.

(9) Pedersen, J. S.; Gerstenberg, M. C. *Macromolecules* **1996**, *29*, 1363–1365.

(10) Baines, F. L.; Billingham, N. C.; Armes, S. P. *Macromolecules* **1996**, *29*, 3416–3420.

(11) Baines, F. L.; Armes, S. P.; Billingham, N. C.; Tuzar, Z. *Macromolecules* **1996**, *29*, 8151–8159.

(12) Triftaridou, A. I.; Vamvakaki, M.; Patrickios, C. S. *Polymer* **2002**, *43*, 2921–2926.

(13) (a) Simmons, M. R.; Yamasaki, E. N.; Patrickios, C. S. *Macromolecules* **2000**, *33*, 3176–3179. (b) Triftaridou, A. I.; Hadjiyannakou, S. C.; Vamvakaki, M.; Patrickios, C. S. *Macromolecules* **2002**, *35*, 2506–2513.

(14) Simmons, M. R.; Patrickios, C. S. *Macromolecules* **1998**, *31*, 9075–9077.

(15) Patrickios, C. S.; Hertler, W. R.; Abbott, N. L.; Hatton, T. A. *Macromolecules* **1994**, *27*, 930–937.

(16) Gao, Z.; Eisenberg, A. *Macromolecules* **1993**, *26*, 7353–7360.

(17) Balsara, N. P.; Tirrell, M.; Lodge, T. P. *Macromolecules* **1991**, *24*, 1975–1986.

(18) Förster, S.; Zisenis, M.; Wenz, E.; Antonietti, M. *J. Chem. Phys.* **1996**, *104*, 9956–9970.

(19) Gindy, M. E.; Prud'homme, R. K.; Panagiotopoulos, A. Z. *J. Chem. Phys.* **2008**, *128*, 164906.